

Methods To Assess Shear-Thinning Hydrogels for Application As Injectable Biomaterials

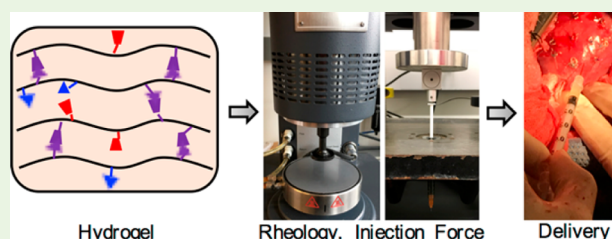
Minna H. Chen,^{†,‡} Leo L. Wang,^{†,‡} Jennifer J. Chung,[§] Young-Hun Kim,[‡] Pavan Atluri,[§] and Jason A. Burdick^{*,‡}

[†]Department of Bioengineering and [§]Division of Cardiovascular Surgery, Department of Surgery, University of Pennsylvania, Philadelphia, Pennsylvania 19104, United States

S Supporting Information

ABSTRACT: Injectable hydrogels have gained popularity as a vehicle for the delivery of cells, growth factors, and other molecules to localize and improve their retention at the injection site, as well as for the mechanical bulking of tissues. However, there are many factors, such as viscosity, storage and loss moduli, and injection force, to consider when evaluating hydrogels for such applications. There are now numerous tools that can be used to quantitatively assess these factors, including for shear-thinning hydrogels because their properties change under mechanical load. Here, we describe relevant rheological tests and ways to measure injection force using a force sensor or a mechanical testing machine toward the evaluation of injectable hydrogels. Injectable, shear-thinning hydrogels can be used in a variety of clinical applications, and as an example we focus on methods for injection into the heart, where an understanding of injection properties and mechanical forces is imperative for consistent hydrogel delivery and retention. We discuss methods for delivery of hydrogels to mouse, rat, and pig hearts in models of myocardial infarction, and compare methods of tissue postprocessing for hydrogel preservation. Our intent is that the methods described herein can be helpful in the design and assessment of shear-thinning hydrogels for widespread biomedical applications.

KEYWORDS: hydrogel, injection, rheology, cardiac, guest–host chemistry



INTRODUCTION

Hydrogels are water-swollen polymer networks with widespread applications in the biomedical sciences, including drug delivery and tissue regeneration.^{1,2} Their high water content and mechanical properties make hydrogels natural mimetics of extracellular matrices. Acellular hydrogels can be delivered for tissue bulking or as artificial tissue mimetics.^{3,4} Hydrogels can also be loaded with cells for therapeutic effect, and may promote additional infiltration of cells upon implantation.^{5,6} Therapeutic molecules can also be encapsulated within hydrogels and released with highly tunable, controlled profiles in response to erosion, swelling, or external stimuli such as enzymes or light.^{7–10}

Over the past few decades, injectable hydrogels have become increasingly popular for their ability to be delivered via minimally invasive approaches.¹ In this context, two major routes for injection have been explored. The first approach is the engineering of hydrogels that gel in situ after injection, through chemical or physical cross-linking mechanisms that occur either during or after injection of the hydrogel precursors.¹¹ Although many hydrogels can be delivered in this fashion, they often require the use of multibarrel syringes for mixing during injection or an external trigger to induce gelation. Gelation is also time sensitive, as cross-linking that occurs too slowly can lead to rapid material dispersion upon injection and prior to gelation, leading to cargo loss.¹² Alternatively,

cross-linking that occurs too quickly can clog the needle or syringe before hydrogel deposition.¹³

To overcome limitations of in situ cross-linking systems, hydrogels have also been engineered to be shear-thinning, which is defined as the ability of a material to decrease in viscosity with increasing shear. Such hydrogels can be preformed into syringes, extruded upon application of shear, and rapidly reform upon cessation of mechanical load, a process known as self-healing. The self-healing nature of these hydrogels allows for improved material retention upon injection and offers advantages to in situ gelation systems, including minimization of potential embolization into the systemic circulation. However, these self-healing systems are often mediated by physical cross-links and may not confer the mechanical stability of in situ cross-linking covalent systems. To overcome this, researchers have explored secondary cross-linking techniques toward stabilizing physically assembled hydrogels after injection.^{4,14}

Shear-thinning and self-healing hydrogels have been investigated in various biomedical applications including drug delivery,^{7,15} tissue regeneration,^{2,16} mechanical bulking,^{3,4,17} and extrusion-based bioprinting.^{18,19} These systems include hydrogels

Received: October 3, 2017

Accepted: November 7, 2017

Published: November 7, 2017

cross-linked through peptide assembly,^{20,21} recombinant protein assembly,^{22,23} ionic interactions,²⁴ thermal assembly,²⁵ electrostatic interactions between colloidal systems,²⁶ and supramolecular chemistry.^{27–31} Dynamic covalent cross-links have also been explored for injection, where their dynamic nature confers shear-thinning during injection and then slow self-healing after injection.^{32,33}

For translation, the injectability of shear-thinning hydrogels plays a major role in enabling minimally invasive delivery (i.e., through percutaneous catheters or via minimally invasive or robotic surgical techniques).^{34,35} For tissue regeneration, the encapsulation of cells within hydrogels also requires specific injection parameters that can influence viability.^{6,36} For bioprinting applications, injection parameters are also important in modulating both the resolution and stability of printed structures, as well as cellular viability.^{37,38} For these reasons, it is important to engineer and tune hydrogels for injection and to understand how various design parameters influence these outcomes, using both quantitative and qualitative techniques. In this methods paper, we detail techniques useful for exploring the mechanical properties that enable shear-thinning and self-healing and demonstrate protocols that can be employed to ensure consistent hydrogel injection and retention.

As a model system, we investigated these properties for hydrogels assembled through guest–host chemistry, which we have previously described, including in a detailed protocols paper on the synthesis of these hydrogel components.^{15,30,39} Specifically, hyaluronic acid (HA) was modified with either β -cyclodextrin (CD, host, 28% of disaccharide repeats) or adamantane (Ad, guest, 22% of disaccharide repeats) to form CD-HA and Ad-HA, respectively, and assembled through supramolecular hydrophobic interactions to form hydrogels that are shear-thinning and self-healing (Figure S1). These materials are only a representative example of the many types of shear-thinning and injectable hydrogels that are available, and the techniques used for their characterization can be applied to other injectable hydrogels. We organize this work into three main methods, including (i) rheological characterization of hydrogels, (ii) measurement of hydrogel injection forces, and (iii) injection of hydrogels into cardiac tissue.

METHOD 1: RHEOLOGICAL CHARACTERIZATION OF HYDROGELS

Rheology is a tool that can be used to quantitatively measure parameters of hydrogels such as viscosity and storage and loss moduli, which are important determinants of hydrogel injectability. Viscosity is a direct measurement of the ability of a material to resist deformation in response to stress, and is a direct measurement of the relative ability of hydrogel formulations to respond to changes in shear stress during injection. Storage and loss moduli provide information about the elastic and viscous response behaviors of a hydrogel, respectively, in response to oscillatory shear. In particular, they measure the extent to which a hydrogel is able to respond to stress and either absorb energy (storage modulus) or undergo stress relaxation to dissipate energy (loss modulus). This information is relevant to better understand the behavior of hydrogels during the injection process.

There are certain steps that must be taken in hydrogel sample preparation, hydrogel loading onto the rheometer, and rheometer data acquisition that are crucial to precise data collection and analysis. In this section, we describe a method for rheological analysis of injectable hydrogels that can be used

to determine compatibility of hydrogels for future injection, including *in vivo* delivery.

Materials. Reagents.

- Adamantane-modified HA (Ad-HA), ~ 22% of repeat units modified, synthesis described elsewhere with reagents available from Sigma (St. Louis, MO)³⁹
- Cyclodextrin-modified HA (CD-HA), ~ 28% of repeat units modified, synthesis described elsewhere with reagents available from Sigma (St. Louis, MO)³⁹
- Phosphate buffered saline (PBS) (Thermo Fisher Scientific, Waltham, MA, cat no: 14190–136)
- Deionized water

Equipment.

- Forceps (e.g., Fine Science Tools, Foster City, CA, cat no: 11008–15)
- 1.5 mL microcentrifuge tubes (e.g., Thermo Fisher Scientific, Waltham, MA, cat no: 05–408–129)
- Vortex (e.g., Thermo Fisher Scientific, Waltham, MA, cat no: 02–215–414) with microcentrifuge tube holder (e.g., Thermo Fisher Scientific, Waltham, MA, cat no: 11–676–363)
- Sonicator (e.g., Branson Ultrasonics, Danbury, CT, model no: CPX5800H)
- Microcentrifuge (e.g., Eppendorf Refrigerated Microcentrifuge 5417R, Eppendorf, Hamburg, Germany)
- Scoopula (made from a cut 1 mL pipet tip)³⁹
- Rheometer (AR 2000 EX, TA Instruments, New Castle, DE)

Procedure. Overview.

- Step 1: Hydrogel preparation
- Step 2: Rheometer setup and calibration
- Step 3: Hydrogel loading onto rheometer
- Step 4: Rheometer data acquisition
- Step 5: Clean-up and next sample preparation
- Step 6: Rheometer data analysis

Step 1: Hydrogel Preparation (2 h). Thaw materials (i.e., Ad-HA, CD-HA) from storage as a dry powder at $-20\text{ }^{\circ}\text{C}$ until they reach room temperature. For guest–host hydrogels, the mixing of Ad-HA with CD-HA in aqueous solution forms an injectable hydrogel. Weigh materials separately into two microcentrifuge tubes and dissolve them in PBS at the desired concentration on a vortex for at least 30 min or until dissolved. Transfer the Ad-HA solution into the CD-HA solution and mix the components with a pipet until the hydrogel is formed. Vortex the hydrogel for 30 min. Then, sonicate the hydrogel for at least 10 min at $50\text{ }^{\circ}\text{C}$ to completely dissolve the hydrogel components. Mix the hydrogel again with a pipet, and then centrifuge for 2 min at 25000 RCF to remove any bubbles. The components and concentrations can be varied depending on the shear-thinning hydrogel that is being investigated.

Critical step: For reproducibility between samples, it is important that the hydrogel components are weighed accurately. It is recommended to prepare solutions of Ad-HA and CD-HA and aliquot these solutions into microcentrifuge tubes so that each tube contains the desired polymer mass. Tubes can then be frozen, lyophilized, and stored under nitrogen until needed. Each aliquot serves as an independent preparation of the hydrogel, and a minimum of three preparations should be tested to investigate the variability in material properties. Additional preparations or technical replicates should be used if large variability is observed between formulations. In addition,

both components of the hydrogel must be thoroughly dissolved and mixed together, without air bubbles. Any inconsistencies in hydrogel preparation will result in poor reproducibility in subsequent experiments.

Step 2: Rheometer Setup and Calibration (15–30 min).

2-1. Rheometer Setup. The following steps are specific to the AR 2000 EX rheometer. These directions are to be taken in addition to steps provided by the manufacturer for rheometer setup and calibration. Close vent and turn on compressor. The pressure should reach 30 PSI for rheometer operation. Connect the geometry and the Peltier plate stage to the rheometer. Depending on the application, the Peltier plate temperature should be set to 25 or 37 °C. For our experiments, the temperature was set to 25 °C, as this is the ambient temperature in which an injection would be performed.

Critical step: Rheometer geometry is important and is determined by sample viscosity, shear rates, and shear stresses desired, as well as sample volumes. For these studies, a cone and plate geometry was chosen because this geometry normalizes shear rates across the entire sample, allowing for an accurate determination of true sample viscosity (as opposed to parallel plate geometries, where shear rates vary across the sample). Cone angle (0° 59' 42") and diameter (20 mm) were chosen based on shear rates and shear stresses desired and to minimize sample volumes needed. The truncation height or gap for this geometry is 27 μm. The gap height must be greater than or equal to ten times the particle size, if particulate-based hydrogels are investigated. Rheometer geometry may need to be adjusted depending on hydrogel properties.

2-2. Calibration. Open the instrument control program on the computer and calibrate instrument inertia, geometry inertia, and bearing friction. Use rotational mapping to calibrate the geometry, then zero the geometry gap to prepare for sample loading.

Critical step: Because the geometry is removed for cleaning after every sample, all calibrations except for the instrument inertia should be repeated between each sample.

Step 3: Hydrogel Loading onto Rheometer (10 min).

Remove the hydrogel from the microcentrifuge tube using a scoopula. Load the hydrogel onto the Peltier plate, taking care not to introduce air or bubbles into the hydrogel. Place the hydrogel in the center of the plate. When centered, use the program to set the height of the cone to the gap height (27 μm). Spin the geometry so that it is turning while it contacts the hydrogel for more even hydrogel flattening (Figure 1a). Either right before (~5% higher) or when the gap height is reached, trim the edges of the hydrogel with a pipet tip so that

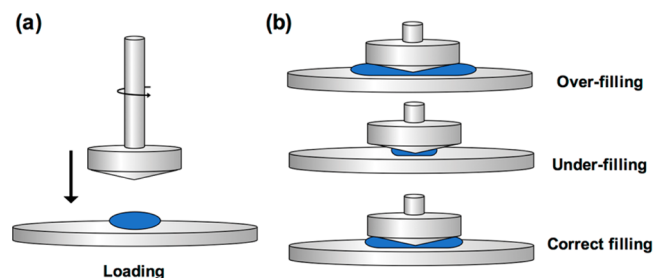


Figure 1. Hydrogel loading onto the rheometer stage. (a) When lowering the geometry onto the hydrogel, spin the geometry slightly for more even hydrogel loading. (b) Over-filling and under-filling of the sample results in increased and decreased forces, respectively. The hydrogel sample must fill the space between the geometry and the rheometer stage correctly for accurate measurements.

the hydrogel correctly fills the geometry (Figure 1b). Place the solvent trap over the geometry and onto the Peltier plate and surround the outer edges of the solvent trap with water to keep the hydrogel hydrated during data acquisition.

Critical step: Correct filling of the geometry by the hydrogel is important for accurate rheological data acquisition. An over-filled sample overestimates mechanical values, while an under-filled sample underestimates mechanical values. A correctly filled sample can be difficult to obtain by trimming. Hydrogel loading volume may need to be optimized based on the geometry used.

Step 4: Rheometer Data Acquisition (Variable). Open the procedure desired and start the protocol. Depending on the tests chosen, the procedure length will vary. For these studies, we used the following protocol:

- A. Time sweep (2 min) at 0.2% strain, 10 Hz
 - a. Note that % strain is determined using strain sweeps to select a % strain lower than the yield strain. A consistently nondeforming strain in our system is <1%. Similarly, the frequency is determined from frequency sweeps by selecting a frequency greater than the crossover frequency.
- B. Frequency sweep from 0.01 to 100 Hz at 0.2% strain with a conditioning time of 3 s, a sampling time of 3 s, and 10 points per decade
 - a. Note that the % strain is the same as for the time sweep.
- C. Time sweep (2 min) at 0.2% strain, 10 Hz to recondition the hydrogel
- D. Strain sweep from 0.01% to 500% strain at 10 Hz with a conditioning time of 3 s, a sampling time of 3 s, and 10 points per decade
 - a. Note that the frequency is the same as for the time sweep.
- E. Low strain (cyclic strain) time sweep (2 min) at 0.2% strain, 10 Hz
- F. High strain (cyclic strain) time sweep (1 min) at 500% strain, 10 Hz
- G. Repeat E, F 5 times for cyclic strain test
- H. Time sweep (2 min) at 0.2% strain, 10 Hz to recondition hydrogel
- I. Continuous ramp from shear rates of 0 to 50 s⁻¹ over 2 min 30 s with 20 points per decade
- J. Continuous ramp from shear rates of 50 to 0 s⁻¹ over 2 min 30 s with 20 points per decade

Step 5: Clean-up and Next Sample Preparation (10 min).

Raise the geometry using controls on the machine. Remove the hydrogel from the stage and clean up any excess water around the solvent trap. Remove the geometry carefully from the bearing and wipe dry. Repeat steps starting at rheometer calibration for all remaining samples.

Critical step: Be sure to clean the stage and complete all calibration steps fully between each sample.

Step 6: Rheometer Data Analysis (Variable). Export data as text files from the computer program. Import files into graphing software and create plots based on tests completed.

Critical step: TA Instruments includes a data analysis program, but this program does not allow you to fully manipulate graphs and graph settings.

Troubleshooting.

- **Air bubbles within hydrogel prior to loading onto rheometer.** After the hydrogel is mixed, spin down the

hydrogel at 25 000 RCF for 2 min to remove any bubbles accumulated during mixing. Note that centrifugation speeds for hydrogels with encapsulated therapeutics should be determined empirically, as small molecules or cells may settle in the hydrogel during centrifugation.

- **Difficulties in hydrogel loading or hydrogel trimming on the rheometer stage.** Change the volume of hydrogel prepared to match the amount of hydrogel that is needed for the specific geometry chosen to limit the need to trim the hydrogel. Take care to load the hydrogel onto the center of the plate and make sure the geometry is slightly spinning when it touches the hydrogel.
- **Hydrogel dries out during testing.** Make sure to add water to the top of geometry and use the solvent trap. Surround the edges of the solvent trap with water to provide a humidified environment for the hydrogel during testing. Lowering the temperature of the Peltier stage may also be helpful for longer studies, as long as the temperature change does not affect the mechanical properties of the hydrogel.

Anticipated Results. For demonstration, we prepared guest–host hydrogels of varying material concentrations for rheological analysis. Using the materials previously described, we formed hydrogels with a total (Ad-HA and CD-HA) polymer content of 5 or 7.5 wt %. Following hydrogel preparation, we loaded these hydrogels onto the rheometer and ran the tests outlined above. The results from these tests are shown in Figure 2. Frequency sweeps (Figure 2a), strain sweeps

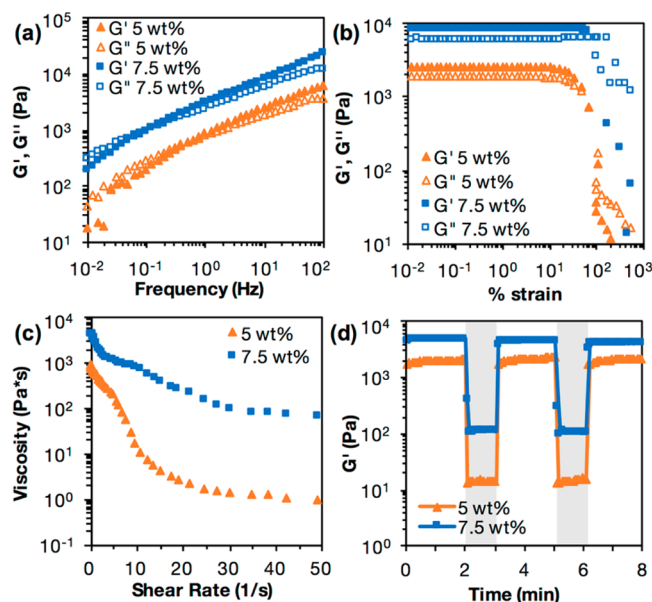


Figure 2. Results of (a) frequency sweep, (b) strain sweep, (c) continuous flow, and (d) cyclic strain time sweep rheology experiments for hydrogels of 5 and 7.5 wt % material concentration, using the described method and rheological parameters. For cyclic strain, shaded regions are high strain (500%) and unshaded regions are low strain (0.2%).

(Figure 2b), continuous flow experiments (Figure 2c), and cyclic strain time sweeps (Figure 2d) are highlighted here.

The frequency sweep indicates that both hydrogels transition from a primarily liquid to a primarily solid state with increasing frequencies, and that the relaxation time for the 5 wt % hydrogel is shorter than that of the 7.5 wt % hydrogel (Figure 2a). Frequency sweeps provide a relative ranking of elastic and

viscous properties under constant strain. Increasing frequencies decrease relaxation times and favor elastic properties (G' , storage modulus) over viscous properties (G'' , loss modulus) as there is minimal time for energy to dissipate or for hydrogels to flow during testing. These results indicate that the 5 wt % hydrogel flows more readily than the 7.5 wt % hydrogel. From the strain sweep, we observe that both hydrogels experience a steep drop in storage and loss moduli after a certain yield strain, indicating material yielding (Figure 2b). This yield strain is lower for the 5 wt % hydrogel, indicating that the 5 wt % hydrogel may be easier to inject than the 7.5 wt % hydrogel.

An important factor for injectability from the rheology data is whether the hydrogel is shear-thinning. Shear-thinning hydrogels experience decreases in viscosity upon application of shear, which are enabled by reversible cross-linking mechanisms. From the continuous flow experiments, we observe that the viscosity decreases as shear rate increases for both the 5 and 7.5 wt % hydrogels, indicating that both hydrogels are shear-thinning (Figure 2c). Similarly, the cyclic strain sweeps show that at high strains, both of these hydrogels yield and show sharp decreases in storage and loss moduli, which are recovered instantly at low strains upon cessation of shear (Figure 2d, Figure S2b, c). This displays the ability of a hydrogel to transition from a predominantly elastic material to a predominantly viscous one, and demonstrates the rapid self-healing properties of this hydrogel. From the continuous flow experiments, we can also observe that the 5 wt % hydrogel displays shear banding, or a precipitous drop in shear stress for certain shear rates (Figure S2a).⁴⁰ This also indicates injectability.

Hydrogels with a lower viscosity and lower storage and loss moduli are typically easier to inject than hydrogels of a high viscosity and high storage and loss moduli. The viscosity of the 5 wt % hydrogel is lower than that of the 7.5 wt % hydrogel, indicating that the 5 wt % hydrogel would be easier to inject (Figure 2c). From the cyclic strain time sweeps, we observe that the storage modulus of both hydrogels change with strain and that the 5 wt % hydrogel has a lower storage modulus than the 7.5 wt % hydrogel, indicating that the 5 wt % hydrogel may be easier to inject (Figure 2d). Cyclic strain time sweeps showing both storage and loss moduli for 5 and 7.5 wt % hydrogels can be found in Figure S2b, c.

METHOD 2: MEASUREMENT OF HYDROGEL INJECTION FORCES

Although material properties such as viscosity, storage modulus, and loss modulus are important for determining injectability, injection force determines whether or not a material is clinically relevant for injection. Controlled methods to measure injection force, such as a force sensor or a material testing machine, allow us to compare quantitatively the injectability of various hydrogels of differing material formulations. In this section, we describe a protocol for determining injection force using both a versatile, inexpensive force sensor and using an established materials testing machine. We also describe factors that influence injection force, such as flow rate, needle gauge, and needle length. Injection force is not only relevant as a physical property but also has effects on hydrogel contents, such as cells.

Materials. Reagents for Hydrogel Formation.

- Adamantane-modified HA (Ad-HA), ~22% of repeat units modified, synthesis described elsewhere with reagents available from Sigma (St. Louis, MO)³⁹

- Cyclodextrin-modified HA (CD-HA), ~28% of repeat units modified, synthesis described elsewhere with reagents available from Sigma (St. Louis, MO)³⁹
- Phosphate buffered saline (PBS) (Thermo Fisher Scientific, Waltham, MA, cat no: 14190–136)

Equipment.

- Forceps (e.g., Fine Science Tools, Foster City, CA, cat no: 11008–15)
- 1.5 mL microcentrifuge tubes (e.g., Thermo Fisher Scientific, Waltham, MA, cat no: 05–408–129)
- Vortex (e.g., Thermo Fisher Scientific, Waltham, MA, cat no: 02–215–414) with microcentrifuge tube holder (e.g., Thermo Fisher Scientific, Waltham, MA, cat no: 11–676–363)
- Sonicator (e.g., Branson Ultrasonics, Danbury, CT, model no: CPX5800H)
- Microcentrifuge (e.g., Eppendorf Refrigerated Microcentrifuge 5417R, Eppendorf, Hamburg, Germany)
- Scoopula (made from a cut 1 mL pipet tip)³⁹
- Various syringes and needles for gel preparation or testing
 - 1 mL syringe (BD, Franklin Lakes, NJ, cat no: 309628)
 - 1/2 mL, 27G x 1/2" tuberculin syringe (BD, Franklin Lakes, NJ, cat no: 305620)
 - 18G x 1/4" needle (McMaster-Carr, Elmhurst, IL, cat no: 75165A121)
 - 25G x 1/4" needle (McMaster-Carr, Elmhurst, IL, cat no: 75165A127)
 - 27G x 1/4" needle (McMaster-Carr, Elmhurst, IL, cat no: 75165A128)
 - 25G x 1 1/2" needle (BD, Franklin Lakes, NJ, cat no: 305127)
- Force Sensor (Tekscan, Boston, MA, FlexiForce Quickstart Board)
- myDAQ Data Acquisition Device (National Instruments, Austin, TX)
- Syringe pump (e.g., New Era Pump Systems Inc., Farmingdale, NY, model no: NE-300)
- Mechanical testing machine (Instron, Norwood, MA, model no: 5848)

Procedure. Overview.

- Step 1: Hydrogel preparation
- Step 2: Hydrogel loading into syringe for testing

- Step 3: Force testing by force sensor or mechanical testing machine

Step 1: Hydrogel Preparation (2 h). Hydrogels are prepared the same way as described for [Method 1](#). Briefly, weigh Ad-HA and CD-HA materials into separate microcentrifuge tubes and dissolve in PBS on a vortex. Mix Ad-HA and CD-HA components together using a pipet. Vortex the hydrogel for 30 min, then sonicate at 50 °C for 10 min. Mix the hydrogel again with a pipet and centrifuge at 25 000 RCF for 2 min to remove entrapped air. Refer to Step 1 of [Method 1](#) for more details and critical steps.

Step 2: Hydrogel Loading into Syringe for Testing (20 min + Overnight Incubation). Cut the needle off of a 1/2 mL, 27G x 1/2 in. tuberculin syringe. Remove the hydrogel from the microcentrifuge tube using a scoopula and load it onto the cut end of the syringe. Pull back on the plunger to load the hydrogel into the syringe. After the hydrogel is loaded, paraffin the open end of the syringe and cut the excess plunger using wire cutters. Centrifuge at 1000 RCF for 3 min to remove bubbles. Then, using the cut portion of the plunger, depress the plunger to load the hydrogel into a 1 mL syringe for testing. We use a 1 mL Luer lock syringe that can be connected to a wide variety of needles with different gauges and lengths. After loading the syringe and attaching the desired needle, wrap the needle with a hydrated wipe and cover with aluminum foil to prevent the hydrogel from drying. Store at 4 °C overnight to allow any remaining bubbles to rise to the top of the syringe barrel.

Critical step: Any imperfections in hydrogel loading and hydrogel preparation (bubbles, dust, etc.) will affect injection force so take care to load the hydrogel into the testing syringe homogeneously. The overnight incubation time is crucial for removing any air taken in during the hydrogel loading process.

Step 3: Force Testing (Variable by Sample Number). *By Force Sensor (Figure 3a).* For best results, use a syringe pump to standardize the application of force to the syringe. Connect the force sensor to myDAQ for data acquisition. For sample MATLAB codes, see [Code S1](#). Create a standard curve by placing weights that correspond to the injection forces that will be measured onto the sensor. Record voltages, and adjust sensitivity of the force sensor if the voltages are out of range. Prime syringes, then place samples onto the syringe pump, and place the force sensor between the plunger of the syringe and the syringe pump. Start the syringe pump and

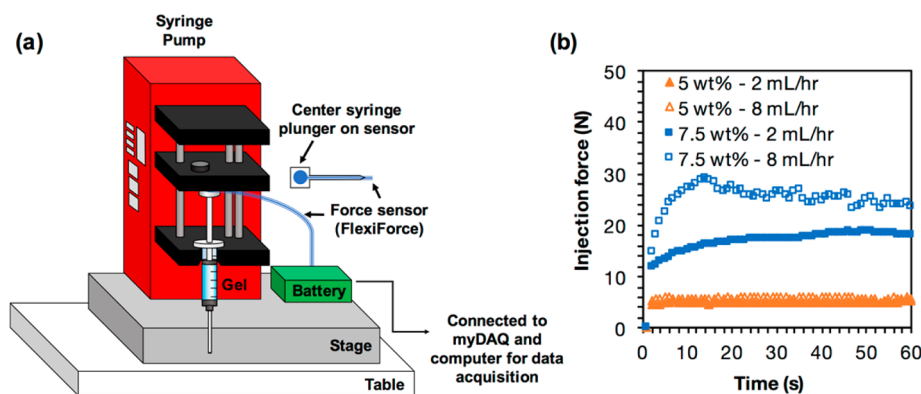


Figure 3. (a) Schematic of the setup for measuring injection force using a force sensor. (b) Plot of injection force over time for hydrogels with varying material concentrations (5 wt %, 7.5 wt %) and different flow rates (2 mL/h, 8 mL/h).

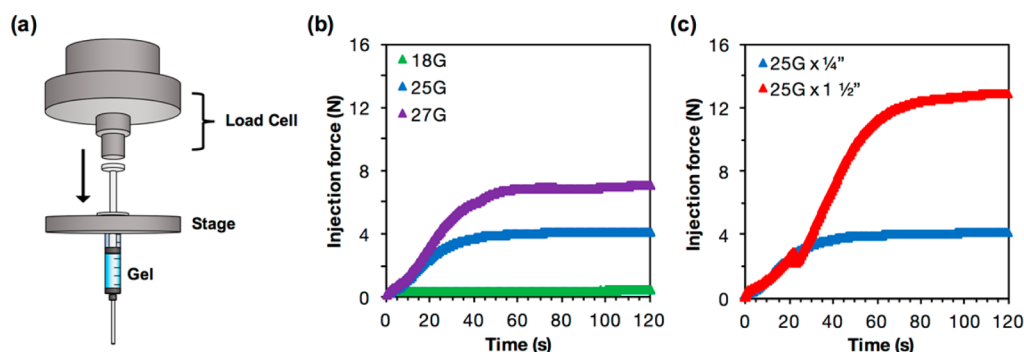


Figure 4. (a) Schematic of the setup for measuring injection force with a mechanical testing machine. (b) Plot showing injection force over time for hydrogels injected from a 1 mL syringe with 1/4 in. needles of 18G, 25G, and 27G. (c) Injection force over time for hydrogels injected from a 1 mL syringe with a 25G needle of 1/4 in. and 1 1/2 in. lengths. All measurements were taken at a flow rate of 2 mL/h.

record voltages for 1–2 min. Convert the voltage to force using the standard curve and plot the force over time.

By Mechanical Testing Machine (Figure 4a). The use of a mechanical testing machine negates the use of a syringe pump, since the load cell will apply even forces. Prime the syringe and place into the stage of the mechanical testing machine. We used the base test frame as a stage with no accompaniments. Zero the force from the load cell and then maneuver the load cell so that it is just touching the syringe, which can be detected by an increase in force. Using the tensile extension mode, set the linear rate to match a flow rate desired for testing. Start applying displacement and record the force over time for 1–2 min. Extract data and plot force over time.

Critical step: For most accurate results, run each trial with the same starting volume of hydrogel. The distance traveled by the plunger will affect the forces applied.

Troubleshooting.

- **Force changes over time.** Over time, injection force should plateau for most hydrogel samples. If the force continues to rise, let the test run for a longer period of time. If the force declines unexpectedly and then increases, there may be imperfections in hydrogel loading. Ensure that the hydrogel is adequately mixed and that there are no bubbles in the testing syringe for the most accurate measurements.
- **Needle detaches from syringe.** Because of the nature of Luer-Lock needles, they can become detached from the syringe upon the application of extreme forces. In these cases, the hydrogel requires a high amount of force for injection. Although this may not be practical for eventual clinical application, to measure this force, use a needle and syringe combination that is not detachable, such as an insulin syringe, to obtain measurements. Note that differences in syringes include barrel diameter, needle gauge, and needle length, all of which are variables that can affect injection force and that need to be controlled between samples for comparison.

Anticipated Results. We tested the injection force necessary to eject both 5 and 7.5 wt % guest–host hydrogels from 1 mL plastic syringes at different flow rates and with differing needle gauges and needle lengths, using both a force sensor and a mechanical testing machine. We observed that, at a flow rate of 2 mL/h, the injection force required for a 5 wt % hydrogel was close to 5N. At the same flow rate, the injection force required for a 7.5 wt % hydrogel was close to 15N (Figure 3b). From rheology we know that the 7.5 wt %

hydrogel has a higher viscosity and a higher storage and loss modulus than the 5 wt % hydrogel, both of which contribute to its higher injection force.

Higher flow rates also lead to higher injection forces, and this effect was dependent on weight percent. For the 5 wt % hydrogels, increasing flow rate from 2 to 8 mL/h minimally increased injection force. For the 7.5 wt % hydrogels, increasing the flow rate from 2 to 8 mL/h increased injection force. Other factors that affect injection force include needle gauge and needle length. Increasing needle gauge, and thereby reducing needle diameter, increased injection force. For a 5 wt % hydrogel with a flow rate of 2 mL/h, reducing the needle diameter from 18G (0.84 mm) to 25G (0.26 mm) to 27G (0.21 mm) increased the injection force from 0.4 to 4 to 7 N, respectively (Figure 4b). We also found that increasing the needle length from 1/4" to 1 1/2" drastically increased injection force for a 5 wt % hydrogel at 2 mL/h from 4N to 13N (Figure 4c). Blips in the force profile as it builds up can be attributed to heterogeneity in hydrogel preparations or improper loading. Care should be taken to ensure hydrogels are adequately mixed prior to testing, and that the syringe is properly loaded to ensure even contact between the load cell and syringe barrel. New syringes and needles should also be used for each independent hydrogel preparation. Single blips may be caused by one of the above issues, but multiple blips within the same profile may indicate problems such as phase separation.

Injection force is not only an important mechanical measure of hydrogel injectability but also affects the ability of the hydrogel to carry certain types of cargo that are sensitive to force, such as cells. When we encapsulated cells within hydrogels using an established protocol, we observed that the viability of cells delivered using a 5 wt % hydrogel was significantly higher than that of cells delivered using a 7.5 wt % hydrogel (Figure S3a, b).³⁹ We determined cell viability after injection using a live/dead assay and CellProfiler to quantify cell counts, as previously described.³⁹ However, not all increases in injection force have a deleterious effect on cargo. When we assessed cell viability after injection at 2 or 40 mL/h, we observed that cell viability was not significantly different at the two flow rates, even though injection force increased with flow rate (Figure S3c–e).

Many factors, such as flow rate, needle gauge, and needle length can affect injection force for the same hydrogel in the same syringe. Using a force sensor or mechanical testing machine to measure injection force can allow for quantifiable measures of injectability that, when other variables are controlled, can be used to compare ease of injection between different hydrogels.

While these tests were done injecting into air, injections into liquids or tissues would more accurately mimic *in vivo* conditions. Clinically relevant injection forces typically are <20 N^{41,42} but actual injectability can depend not only on force but also on the ergonomics of the syringe, which can affect the force applied. The methods described here for characterizing injectable hydrogels using rheology and measurements of injection force can also be utilized for applications other than *in vivo* delivery that include ejection of hydrogels, such as 3D printing.

Additional Consideration: Qualitative Assessment of Hydrogel Injectability. Although quantitative assessments of parameters are important for evaluating injectability, we recommend assessment of injections *in vitro* and *ex vivo* prior to any *in vivo* application. Using techniques previously described for loading hydrogels into syringes, we suggest injecting hydrogels into PBS, a buffer mimicking physiological pH and osmolarity. Injections into PBS allow for the assessment of the forces required to manually extrude hydrogels from syringes with various parameters, and for the assessment of self-healing after injection. A dye can be used to visualize hydrogels during these assessments. For self-healing materials, hydrogels are expected to retain their shape after injection and, if dyed, should not lead to dispersion of polymer or dye into the PBS solution. Here, we demonstrate injections of guest–host-modified HA (green) or polyethylenimine (PEI, red) hydrogels into PBS, where both demonstrate rapid self-healing after injection with no dispersion of payload (Figure 5a).

Ex vivo experiments may also play an important role in understanding self-healing and retention after injection. In our example, we used explanted porcine cardiac tissue as an *ex vivo* model for *in vivo* injections, and injected both HA and PEI hydrogels into the tissue. Following injection, tissue can be incubated in PBS and imaged using techniques such as MRI (Figure 5b). A variety of methods exist to visualize or reconstruct MRI data into 3D images that allow for quantification of hydrogel retention or shape (Figure 5c).⁴³ Injections of hydrogel into *ex vivo* tissue are important for measuring hydrogel retention, distribution, swelling, and leakage after delivery, all of which are important to understand for predicting hydrogel behavior in dynamic, *in vivo* systems.

■ METHOD 3: INJECTION OF HYDROGELS INTO CARDIAC TISSUES

Although hydrogels have been investigated *in vivo* in various types of tissue, one area in which injectable hydrogels have been widely investigated is cardiac tissue,^{3,4,35,44} and there are

several hydrogel formulations that have undergone testing in clinical trials (NCT01311791, NCT02305602). Here, hydrogels are used for mechanical bulking,^{3,4,35} modulating remodeling,^{7,17} or therapeutic delivery (cells, small molecules, RNAs) after infarction.^{6,15,45} An additional advantage of injectable hydrogels in cardiac disease is the potential to deliver material through minimally invasive approaches, such as percutaneously through a catheter.^{34,35} Toward their assessment *in vivo*, hydrogels have been used in small and large animal models in which they are injected intramyocardially into the infarct or into the border zone around the infarct. Although delivery through catheters has been investigated in larger animal models, most current models of hydrogel injections are still through thoracotomy and myocardial injection, which is an open-heart surgery and will be the focus of this section.

To implement hydrogel injections in models of infarction, investigators should understand differences between various animal models, when they are used, and their implications for intramyocardial hydrogel injections. Here, we outline the steps necessary for injection of hydrogels into small and large animal models of myocardial infarction. These protocols focus on the injection of hydrogels, and additional protocols regarding the surgeries themselves (anesthesia, intubation, thoracotomy, closure, and postoperative care) can complement these methods.^{46–49} We have found that the steps listed below lead to reproducible and reliable hydrogel injection models. However, these steps should be used as guidelines for other hydrogel injections and can be adapted as necessary on a case-by-case basis, where variations in the method (e.g., location, number, volume, or timing of injections) are desired. We note that investigators should obtain IACUC or similar approval and training prior to animal testing.

■ SMALL ANIMAL CARDIAC INJECTIONS

The small animal cardiac models we employ for assessment of our injectable hydrogels are mouse and rat. While the mouse has been a model organism for studying heart disease, it is also the farthest from translatability to humans due to its small size. The main advantage is in the use of transgenic mice that allow for lineage tracing strategies or other gene manipulation techniques that can lead to dilated, hypertrophic, autoimmune, or other models of heart failure.^{50,51} Because the majority of human genes have murine orthologs, the roles of pathologic targets in humans can be studied at an accelerated pace in mice. However, mouse models of infarction are technically challenging, requiring significant expertise given the mouse myocardium is

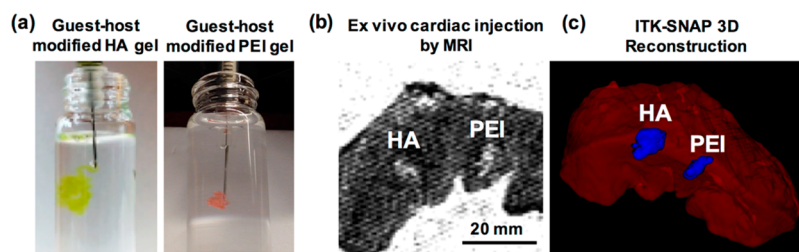


Figure 5. *In vitro* and *ex vivo* injections from 27G \times 1/2 in. tuberculin syringes. (a) Manual injections of guest–host-modified HA hydrogels (green) or PEI hydrogels (orange) injected into PBS from 27G \times 1/2 in. tuberculin syringes, demonstrating retention of dye and no dispersion of material after injection. (b) T2 weighted MRI visualization of HA and PEI hydrogels 24 h after injection into porcine cardiac tissue. Tissue was submerged in PBS for 24 h before imaging. (c) 3D reconstruction of hydrogel plugs from ITK-SNAP using automated segmentation with manual edge correction in porcine cardiac tissue *ex vivo* after injection.

very thin, which can complicate injection.⁵² Moreover, the small size of the mouse heart leads to limited tissue post-mortem for histological analysis. Rats are larger than mice and are used because they enable easier hemodynamic modalities (such as pressure–volume catheterization) to assess cardiovascular function, and surgical techniques are often technically easier than in mice, leading to decreased noise and variability in studies. Rat studies also enable greater quantities of myocardial tissue for post-mortem histological analyses.⁵³ However, costs associated with rat models may be higher and favorable results may not always be reproducible in clinical studies. Moreover, although transgenic rat models exist, a high cost is associated with generating and maintaining these colonies and there are appreciably fewer models in rats than in mice.^{47–50}

Materials. Reagents.

- Adamantane-modified HA (Ad-HA), ~ 22% of repeat units modified, synthesis described elsewhere with reagents available from Sigma (St. Louis, MO)³⁹
- Cyclodextrin-modified HA (CD-HA), ~ 28% of repeat units modified, synthesis described elsewhere with reagents available from Sigma (St. Louis, MO)³⁹
- Phosphate buffered saline (PBS) (Thermo Fisher Scientific, Waltham, MA, cat no: 14190–136)
- Analgesics as listed below or a comparable and approved pain control regimen
 - Meloxicam (Norbrook Laboratories, Newry, United Kingdom, 5 mg/mL solution for injection)
 - Buprenorphine (ZooPharm, Windsor, CO, 1 mg/mL)
 - Bupivacaine (Hospira, Inc., Lake Forest, IL, 0.25%, 2.5 mg/mL)
- Betadine solution swab stick (Purdue Pharma LP, Stamford, CT)
- Isoflurane (Piramal Enterprises Ltd., Mumbai, India, 250 mL)

Equipment.

- Hydrogel preparation
 - Forceps (e.g., Fine Science Tools, Foster City, CA, cat no: 11008–15)
 - 1.5 mL microcentrifuge tubes (e.g., Thermo Fisher Scientific, Waltham, MA, cat no: 05–408–129)
 - Vortex (e.g., Thermo Fisher Scientific, Waltham, MA, cat no: 02–215–414) with microcentrifuge tube holder (e.g., Thermo Fisher Scientific, Waltham, MA, cat no: 11–676–363)
 - Sonicator (e.g., Branson Ultrasonics, Danbury, CT, model no: CPX5800H)
 - Microcentrifuge (e.g., Eppendorf Refrigerated Microcentrifuge 5417R, Eppendorf, Hamburg, Germany)
 - Scoopula (made from a cut 1 mL pipet tip)³⁹
 - 1/2 mL, 27G × 1/2 in. tuberculin syringe (e.g., BD, Franklin Lakes, NJ, cat no: 305620)
 - 1/2 mL, 28G × 1/2 in. insulin syringe (e.g., BD, Franklin Lakes, NJ, cat no: 329420)
- In vivo mouse or rat surgery setup^{46,54}
 - Mouse/rat ventilator with isoflurane (Isoflurane VIP 3000 Vaporizer, Midmark Co, Dayton, OH; Anesthesia workstation, Halowell EMC, Pittsfield, MA, cat no: 000A5653)

- Endotracheal tube
 - Mice: 20G × 1 1/4 in. IV catheter (NIPRO, Bridgewater, NJ, Nipro Safelet IV Catheter)
 - Rats: 16G × 2 in. IV catheter (Terumo, Tokyo, Japan, Surflo IV Catheter)
- Electrical clippers/shaver (Wahl Clipper Co, Sterling, IL)
- 45° Angled Potts scissors (Teleflex, Wayne, PA, Pilling 35–2166 N22)
- Blunt-tip scissors (Integra Miltex, York, PA, cat no: 5-SC-16)
- Blunt-tip forceps (Integra Miltex, York, PA, cat no: 6–30)
- Eye retractor (for mice, Integra Miltex, York, PA, cat no: 11–12)
- Weitlaner retractor (for rats, Fine Science Tools, Foster City, CA, cat no: 17012–11)
- Sutures (Medtronic, Fridley, MN, for mouse ligation: SurgiPro II 8–0 VP-900-X, rat ligation: SurgiPro II 7–0 VPF-702-X, closing: SurgiPro II 4–0 VP-583-X)
- Sterile gauze (Thermo Fisher Scientific, Waltham, MA, cat no: 22–362–178)

Procedure. Overview.

- Step 1: Hydrogel preparation and syringe loading
- Step 2: Anesthesia
- Step 3: Infarct induction
- Step 4: Syringe inspection
- Step 5: Syringe priming
- Step 6: Stay suture placement
- Step 7: Needle insertion
- Step 8: Hydrogel extrusion
- Step 9: Needle withdrawal

Step 1. Hydrogel Preparation and Syringe Loading (2 h).

Polymers should be sterilized under germicidal UV irradiation for at minimum 30 min and subsequently dissolved in sterile PBS solution and loaded into syringes as previously described.³⁹ Cells or therapeutics that are to be encapsulated should be included at this step. Hydrogels should be kept on ice if biologics are included. For mice, up to 10 μ L of gel are typically injected per animal, with no more than 5 μ L per injection site. In rats, depending on the hydrogel properties, 50–100 μ L can be injected in 20 μ L increments. Hydrogels are usually prepared for a single mouse or rat in a 1/2 mL, 1/2 in., 27G or 28G insulin or tuberculin syringe (Figure 6a). Separate hydrogels should be made for each animal to maintain sterility and avoid cross-contamination.

Step 2. Anesthesia (5 min). A method of anesthesia should be selected in accordance with animal health and safety protocols. In our animal models, mice or rats are anesthetized under 1–3% isoflurane, intubated with an endotracheal tube, and maintained under 1–3% isoflurane and positive pressure ventilation.

Step 3. Infarct Induction (5 min). The animal should be placed in right lateral recumbency. Shave the left anterior and lateral thorax and disinfect with iodine. Incise the skin and subcutaneous tissues with heavy scissors to expose the ribcage. The thoracic cavity should be entered between the fourth and fifth ribs in the fourth intercostal space. Using the forceps to grab the fourth rib, elevate the ribcage to provide room between the chest wall and underlying heart and lungs and carefully insert one blade of the Potts scissor, taking care not to injure the intrathoracic structures. Extend the incision to

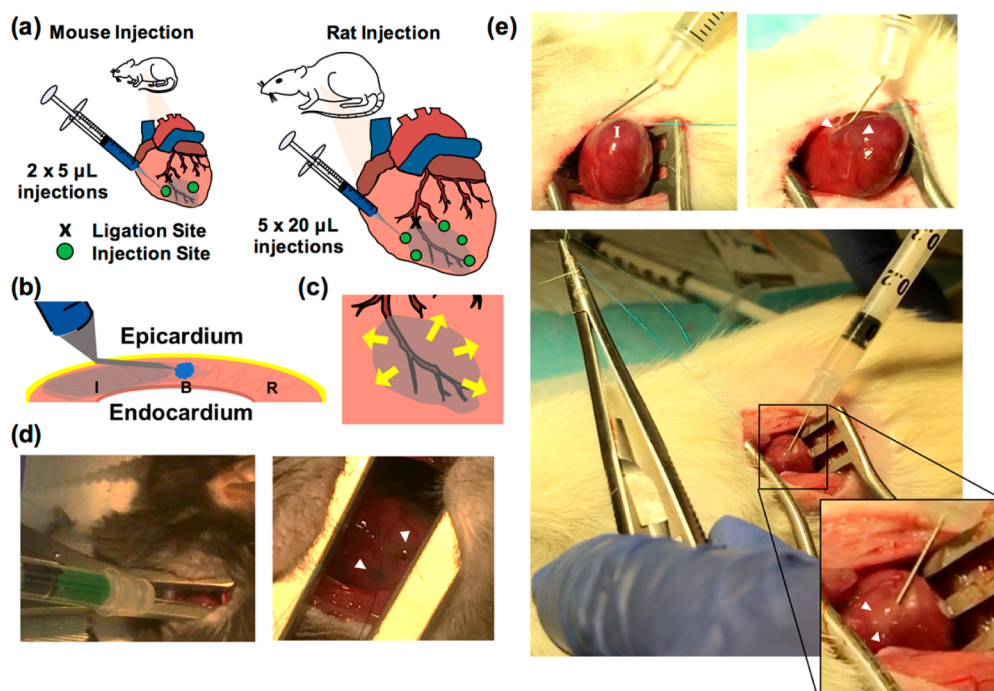


Figure 6. Intramyocardial hydrogel injections in mouse and rat models. (a) Schematic of ligation and injection sites in mouse and rat models. A representative mouse model uses $2 \times 5 \mu\text{L}$ injections lateral to the border zone, and rat models use $5 \times 20 \mu\text{L}$ injections circumferentially around the infarct. (b) Technique for localizing gel to infarct border zone, where needle is angled and inserted into the infarct as parallel as possible to the tissue. With the bevel pointing upward toward the epicardium, the hydrogel remains in constant view of the operator. (c) Schematic of injection sites and direction of arrow insertion in a radial pattern for targeting of the border zone in a rat infarct model. (d) Injection of HA hydrogel into a mouse heart and subsequent visualization. (e) Injection of HA hydrogel into a rat heart, demonstrating needle angling, stay suture placement, heart elevation from the thoracic cavity, and hydrogel localization.

provide adequate exposure to the heart. Place the retractors between the cut ribs and spread carefully to achieve visualization of the target organ. Using blunt forceps, lift the pericardium off the surface of the heart and cut a generous window into the tissue using blunt-tip scissors.⁴⁶ Using anatomic landmarks, identify the artery of interest and perform a suture ligation of a major arterial branch in as consistent a manner as possible to ensure relatively reproducible regions of infarction. This is traditionally done through ligation of the left anterior descending artery, 1–2 mm below the level of the left atrial appendage (Figure 6a).⁵⁴

Step 4. Syringe Inspection (<1 min). Inspect the syringe for damage and air bubbles, and ensure that adequate volumes have been prepared for injection.

Critical step: Air bubbles in the hydrogel have the potential to cause embolization. Thus, routine inspection of syringes for air bubbles and subsequent centrifugation is necessary.

Step 5. Syringe Priming (<1 min). Prime the syringe by manually applying pressure until the hydrogel begins to extrude from the needle. It is important to be familiar with the forces required prior to the cardiac injection.

Step 6. Stay Suture Placement (5 min). Using a stay suture or the ligation suture, manually orient the heart so that the injection site is in clear view of the operator. This may require externalizing the heart from within the chest cavity, especially for posterior injections that would otherwise be inaccessible. Use gentle and controlled movements to prevent tearing of the myocardium and bleeding.

Step 7. Needle Insertion (<1 min). While stabilizing the heart in the desired position, insert the needle tip either parallel or as close to parallel to the injection site as possible, avoiding

any visible surface vessels. It may be necessary to introduce a gentle bend in the needle to achieve the appropriate angle for insertion (0–45 degrees). This step ensures that any penetration by the needle does not lead to ventricular puncture (Figure 6b).

Critical step: Throughout the duration of needle insertion, the needle tip should remain superficial enough to be visible to the operator through the overlying myocardium. The bevel should always be inserted face up in clear view of the operator so that it is apparent when the hydrogel begins to extrude. During the hydrogel injection, a visible wheal should form at the needle tip. If not visible, the needle has been inserted too deep and should be repositioned.

Critical step: To target the border zone, the needle should be inserted into the infarct and directed radially into the border zone. This improves targeting as the infarct is akinetic, allowing for easier insertion. This also minimizes any potential damage from the needle to noninfarcted myocardium (Figure 6c).

Step 8. Hydrogel Extrusion (<1 min). After ensuring that the entire length of the bevel is buried within tissue, inject slowly with controlled, manual pressure until adequate volumes have been injected. We recommend one hand be used to stabilize the needle in the heart while the other is used to inject material (Figure 6d, e, Video S1 and Video S2).

Step 9. Needle Withdrawal (<1 min). After the injection is complete, wait for 1–2 s before withdrawing the needle so that the hydrogel can disperse into the tissue. Withdraw the needle slowly to prevent material leakage. Manual pressure can be applied after injection also to limit material leakage.

Troubleshooting.

- **Hydrogel cannot be visualized during injection.** The needle is inserted too far into the tissue, which increases

likelihood of ventricular puncture and embolization. Remove the syringe and reinsert as needed. If bleeding occurs, apply manual pressure with gauze until bleeding stops.

- **Hydrogel causes excessive bleeding or damage.** This is an unlikely scenario where there has likely been damage to the ventricle caused by needle movement during placement or injection. To prevent this, it is important that the hand controlling the syringe be rested on a solid immobile surface to prevent small movements during needle insertion and injection. A controlled injection using two hands, one to stabilize the syringe in the heart and one to apply pressure, may be necessary for some operators. If this occurs, gentle compression with a dry gauze will most often achieve hemostasis.
- **Hydrogel leaking from injection sites.** This can occur when needles are too quickly removed following injection or if the hydrogel used has slow self-healing properties. To prevent this, slowly withdraw the needle from the injection site 1–2 s after the injection is complete. Manual pressure can be applied over the hydrogel as the needle is withdrawn. Occasionally, this is due to the bevel not being fully inserted into the tissue during the injection. In this case, reinsert the needle and ensure that the bevel is fully buried within the tissue. Leaked hydrogel can be easily wiped away with a gauze pad.

■ LARGE ANIMAL CARDIAC INJECTIONS

Pig and to a lesser extent sheep hearts exhibit anatomy similar to that of humans and are much more relevant models for assessing hydrogel injections and effects of encapsulated therapeutics, although we note there is still variance in coronary anatomy from animal to animal.^{55,56} For infarct models, it is imperative to select reproducible models that promote consistently equal-sized infarcts in the same location. Typically, this involves manipulation and standardization of one or more accessory vessels and surgeons must be knowledgeable about cardiac anatomy. The decision between pig and sheep is largely one of preference, as they are both structurally similar and mimic human anatomy, although we note that pig valves are used as xenografts in the human heart. Pigs are predisposed to arrhythmias, and precautions must be taken to avoid them or treat them. Sheep are prone to zoonotic disease, and may be more difficult to image because of their anatomy.⁵⁵ Because the myocardial infarction model in large animals is complex both medically and surgically, we have only included the steps here that are relevant to hydrogel injections following thoracotomy and exposure of the heart. Well-described protocols for preparation of animals for large animal myocardial infarctions should be used to supplement these methods.^{47–49} With protocol modification, the hydrogel can be injected soon after infarction or at a later time point, depending on the stage of remodeling that is desired for treatment. Also, hydrogel preparation and syringe loading is the same for large animal models as described in Step 1 for small animal models.

Materials. Reagents.

- Hydrogels prepared in 1/2 mL, 27G × 1/2 in. tuberculin syringes (e.g., BD, Franklin Lakes, NJ, cat no: 305620) or 1/2 mL, 28G × 1/2 in. insulin syringes (e.g., BD, Franklin Lakes, NJ, cat no: 329420), with one syringe per injection site
- Titanium markers

Equipment.

- Sheep or pig surgery setup^{47–49}

Procedure. Overview.

- Step 1: Infarct induction and closure if necessary
- Step 2: Syringe inspection
- Step 3: Syringe priming
- Step 4: Marker placement
- Step 5: Needle insertion
- Step 6: Hydrogel extrusion
- Step 7: Needle withdrawal

Step 1. Infarct Induction and Closure if Necessary (1 h).

An example pig infarction model consists of ligation of three obtuse marginal branches (OM1, OM2, OM4) of the left circumflex artery and a diagonal branch (D1) of the left anterior descending artery to create a reliable infarct size of ~20% (Figure 7a). Alternative strategies to induce infarction such as occlusion of the left circumflex exist, and these should be considered on a case-by-case basis. Titanium markers are placed to surround the infarct site for delineation of infarct. These markers are sutured into the tissue (up to 6–10, depending on infarct size). It is important that these markers be made from a nonferromagnetic metal so that they do not prohibit subsequent MRI analyses. Hydrogel injections can then be made immediately after infarction or at a later time point, in which case the thoracotomy should be closed. In this example model, hydrogel injections are made 3 days after ligation and infarct induction.

Step 2. Syringe Inspection (<1 min). Inspect the syringe for damage and air bubbles, and ensure that adequate volumes have been prepared for injection.

Critical step: Air bubbles in the hydrogel have the potential to cause embolization. However, because of the sensitivity of large animals to environmental sterility, we suggest the preparation of extra replacement syringes with hydrogels. Typically 1–2 replacement syringes are prepared per animal.

Step 3. Syringe Priming (<1 min). Prime the syringe by manually applying pressure until hydrogel begins to extrude from the needle. It is important to be familiar with the forces required prior to the cardiac injection.

Step 4. Marker Placement (10 min). Prior to hydrogel injections, place titanium markers over the planned injection sites for post-mortem histological analyses. These should be sutured into the tissue as described in Step 1. (Figure 7b).

Step 5. Needle Insertion (<1 min). Insert the needle tip either parallel or as close to parallel to the injection site as possible (0–45°). Again, it may be necessary to introduce a gentle bend in the needle to achieve the appropriate angle for insertion (0–45°). This step ensures that any accidental penetration by the needle does not lead to ventricular puncture or hydrogel injection into the ventricle. For large animal models with thicker ventricular walls, the needle can also be inserted perpendicular to the tissue with a foam spacer to prevent ventricular puncture (Figure 7c).

Critical step: Because infarct tissue will thin over time as the heart dilates after infarction, the ability to insert the needle perpendicularly without overpenetration depends on when the injections are performed. If immediately after infarct induction, the ventricle is still thick and overpenetration is unlikely. If weeks after infarct induction, the ventricle is likely thin and fibrotic and needles may overpenetrate easily. In these cases, the syringe should be inserted as close to parallel to the tissue as possible.

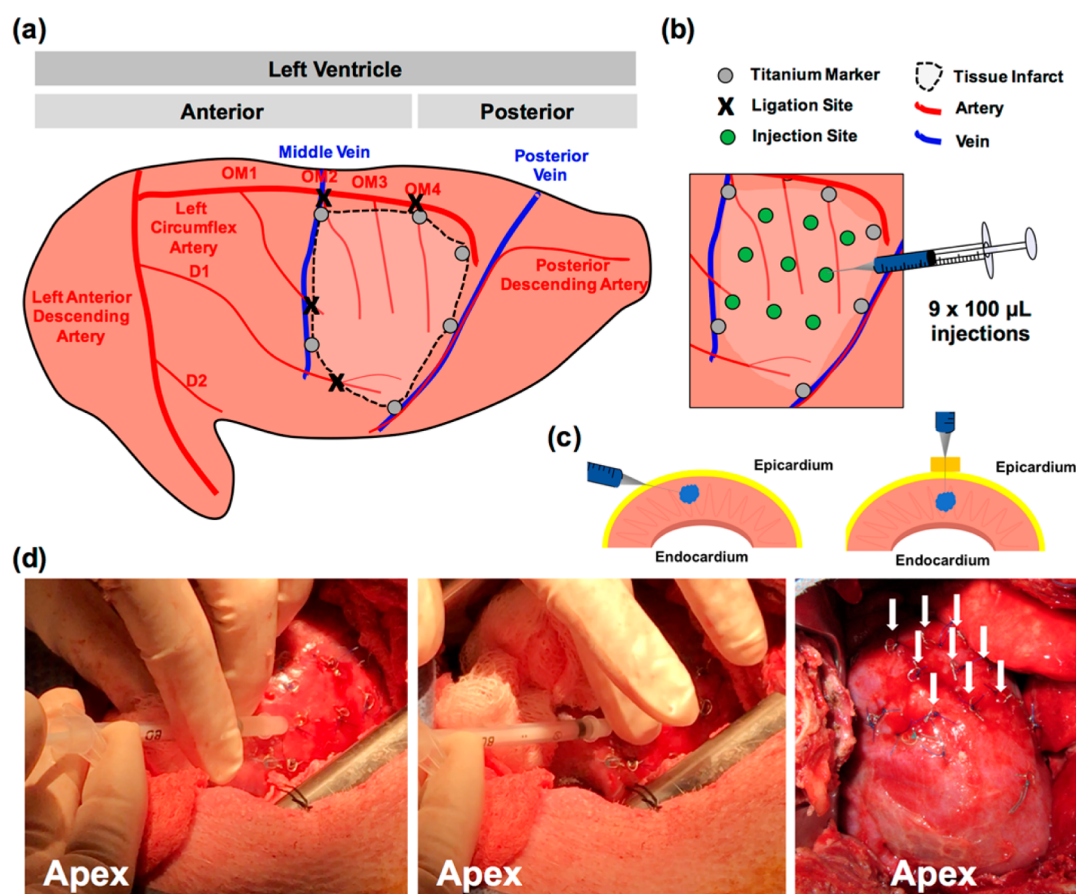


Figure 7. Intramyocardial hydrogel injection in a pig model of myocardial infarction. (a) Schematic of ligation sites in obtuse marginal branches of the left circumflex artery and diagonal branches of the left anterior descending artery. Titanium markers are placed circumferentially around the infarct for visualization after injection. (b) Traditional injection model for porcine infarct models, consisting of $9 \times 100 \mu\text{L}$ injections. Titanium markers are placed over injection sites prior to hydrogel injection to ensure consistent spacing and to avoid vasculature during injection. (c) Techniques for injection into porcine tissue. Angling the needle parallel to myocardium will allow for penetration directly into myocardium without injection into the ventricle. A foam spacer can also be placed on the needle to permit injection directly into the epicardium without angling the needle. (d) Photos of injection, demonstrating needle position and hydrogel injection into sites marked by titanium markers, finger placement to prevent leak of material after injection as the needle is withdrawn, and 9 injection sites marked by titanium markers following injection into the infarct.

Step 6. Hydrogel Extrusion (<1 min). Inject slowly with controlled, manual pressure until adequate volumes have been injected (Figure 7d, Video S3). Injecting slowly allows the hydrogel to better disperse into the tissue. Injecting too rapidly can cause the hydrogel to leak from the injection site.

Critical step: Hydrogel injection into the infarct (especially at earlier time points) is challenging due to the degree of movement intrinsic to the cardiac cycle. It is important to establish a technique that allows the needle to be maintained in the same location during the injection that is not affected by movement of the heart. One technique to overcome this is to place sterile gauze pads under and/or around the heart to limit movement. Once the needle has been inserted, hydrogels should be injected immediately.

Step 7. Needle Withdrawal (<1 min). After the injection is complete, manually apply pressure over the injection site with a finger as the needle is withdrawn or after the needle is withdrawn to prevent material leakage (Figure S5).

Critical step: Placing a finger over the injection site as the needle is withdrawn or after the needle is withdrawn is needed due to the large volumes that are injected in larger animal models. Negligence here will result in inconsistent injections. Leaked gel can be wiped away with a gauze pad. Anisotropy in

the heart means certain injection sites are more susceptible to leaking than others.

Troubleshooting.

- **Excess bleeding during injection.** Recognition of coronary landmarks and major vascular structures can help to prevent bleeding during injection. If blood vessels are entered, this can increase risk for both bleeding and embolization. Major venous and arteriolar structures are visible to the naked eye so operators should examine the heart for such structures before injections are made.
- **Hydrogel leakage from injection sites.** When hydrogel leakage is observed, injection should be done slower. Allow the needle to remain in the tissue for several seconds after injection, then withdraw the needle slowly with manual pressure placed by a finger over the injection site. If this continues to be a problem, place a finger over the injection site above the needle tip during the injection itself. Leaked gel can be wiped away by a gauze pad. Sites where the hydrogel leaks should be recorded.

Additional Consideration: Hydrogel Processing after Cardiac Injection. In addition to assessing functional outcomes of cardiac remodeling after MI, most studies involve investigating tissue outcomes of cardiac remodeling. These outcomes

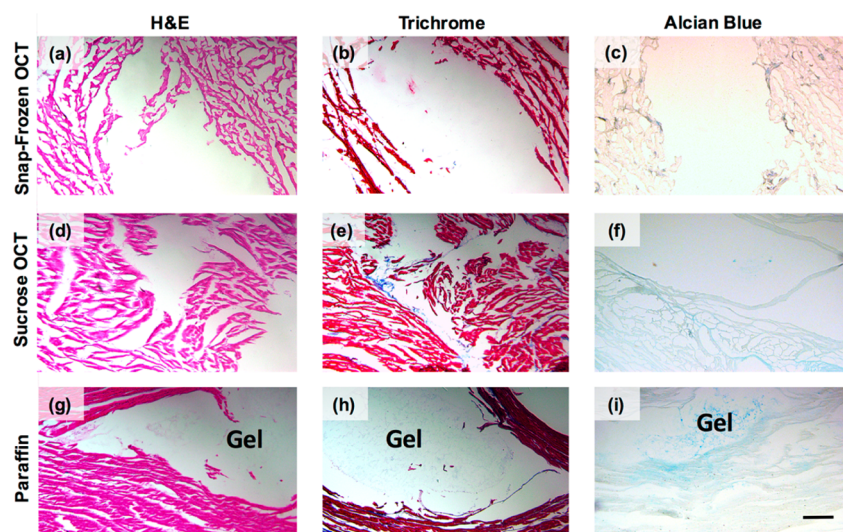


Figure 8. Hydrogel and tissue preservation after embedding, sectioning, and staining. Ex vivo tissue after being (a–c) snap-frozen in OCT, (d–f) frozen in OCT following sucrose infiltration, or (g–i) embedded in paraffin. (a, d, g) H&E, (b, e, h) Masson’s Trichrome, and (c, f, i) Alcian Blue staining was performed to visualize the hydrogel within the tissue. Scale bar: 200 μm .

are often measured through stains, such as Masson’s Trichrome, to assess collagen content and scar fraction, as well as immunohistochemistry. All of these outcomes involve a tissue preservation step, followed by sectioning, and then a staining process. Because of the weak mechanics and hydrophilicity of hydrogels described in these methods, typical processing can be challenging. Guest–host hydrogel was injected into ex vivo porcine cardiac tissue and then, for preservation, was embedded into OCT either via snap-freezing (Figure 8a–c) or via freezing after sucrose infiltration (Figure 8d–f). Tissue was also embedded in paraffin (Figure 8g–i). Next, to compare hydrogel and tissue morphology after tissue preservation, we performed hematoxylin and eosin (H&E), Masson’s Trichrome, and Alcian blue stains.

Tissue preservation was poorest in snap-frozen OCT samples, and improved in sucrose infiltration samples. Sucrose infiltration prevents tissue expansion during freezing, which can help reduce tissue artifacts. However, tissue morphology was most preserved in paraffin-embedded samples. The same trends followed for hydrogel morphology. Hydrogel was not observed at all in the snap-frozen OCT samples or sucrose infiltration samples, and was only visible in the paraffin-embedded samples. Alcian blue was used to confirm the presence of glycosaminoglycans, such as the hyaluronic acid we would expect from our hydrogel, on the slides.

Because paraffin embedding completely dehydrates the tissue and the hydrogel, it decreases the likelihood that the hydrogel will be washed away in subsequent staining steps, even if it is preserved after sectioning. Placing paraffin slides into a 37 $^{\circ}\text{C}$ oven for 15 min prior to staining can help completely remove any remaining water beneath the tissue and the slide, effectively securing the tissue to the slide. However, paraffin embedding is much more tedious than the other methods. Snap-freezing is the fastest (only a few hours), followed by sucrose infiltration (3 days), and then paraffin embedding (4–6 days, depending on tissue size). For paraffin embedding, it is crucial to allow each of the many solutions to fully diffuse within the tissue, which can take days. Still, we recommend paraffin-embedding tissue when it is preferred to preserve the hydrogel within the tissue sections.

Additional Consideration: Hydrogel Injection into Other Tissues. Injectable hydrogels maintain great utility

outside of the heart due to their applicability for tissue engineering and drug delivery. Whereas every organ will necessitate its own protocols for injection, there are several considerations that can be generalized toward other organs and tissues.

Dynamic tissues may necessitate different hydrogel properties. Hydrogels injected into load-bearing tissue like the knee joint may require additional mechanical properties, like toughness, in order to respond to cyclic loading.^{57,58} The ability to confer such mechanics may limit injection, and thus adequate quantitative and qualitative assessments are necessary. Kinetic tissue like the heart, skeletal muscle, or joints may have higher clearance rates in vivo, and these properties should also be assessed quantitatively in vitro and in vivo.

Hydrogel swelling should also be considered. High swelling rates may elevate pressures in closed environments, potentially leading to elevated intracranial pressure and complications such as edema, herniation, or cauda equina in the central nervous system⁵⁹ or elevated intraocular pressure for intravitreal injections in the eye.⁶⁰ Uncontrolled swelling can also compress nearby tissue and compromise blood and lymphatic flow.⁶¹ These properties should be measured in vitro prior to hydrogel injection in vivo. The use of nonswelling injectable hydrogels may be better suited for such applications.

Avoiding vasculature during hydrogel injection is also important, as major bleeding events or embolization may occur if materials are injected too close to vascular structures. Embolization events continue to be a complication even for clinically-approved, injectable materials.⁶² Thus, knowledge of vascular anatomy is crucial for proper injection techniques. For cardiac injections, angiography can be used to visualize coronary anatomy.

■ SUMMARY

Injectable hydrogels are useful delivery vehicles and have been used in many clinical applications to improve cargo retention at the injection site. Using rheology and injection force measurements to characterize these hydrogels can be helpful to determine which material formulation is best suited for an application, as long as considerations are taken to carefully prepare hydrogel samples for accuracy and reproducibility. However, it can be

difficult to definitively establish minimum or maximum values for viscosity or storage and loss moduli, for example, that will render the hydrogel to be injectable, since those values will vary depending on the shear forces applied. While it may be easier to define clinically relevant limits for injection force, every clinician will handle these hydrogels differently and the maximum amount of force a clinician can apply will depend also on the ergonomics of the syringe.

More qualitative techniques, such as *in vitro* injections into water or *ex vivo* injections into tissue can provide even more information about how an injectable hydrogel will behave *in vivo*, providing insight into qualities such as gelation time, swelling, and hydrogel retention. Characterizing an injectable hydrogel prior to conducting *in vivo* experiments in these ways can help researchers avoid challenges they would otherwise encounter later, such as slow gelation times that lead to hydrogel leakage or stiff hydrogels that are impossible to inject with control by hand.

For delivery *in vivo*, special care must be taken both to avoid damage to healthy native tissue during injection and to retain the hydrogel in the delivery site. These considerations are especially important for cardiac delivery, where mechanical forces can make it difficult to control injection and to localize the hydrogel where desired. We describe techniques here that can be used for cardiac delivery in mouse, rat, and pig animal models, as well as considerations for tissue postprocessing if hydrogel visualization is desired. Paraffin embedding of tissues, although time-intensive, best preserves hydrogel morphology by removing water which can make the hydrogel susceptible to washing during staining.

In conclusion, we describe here quantitative and qualitative *in vitro* techniques for characterizing injectable hydrogels. These techniques can be valuable for exploring the capabilities of an injectable hydrogel or comparing formulations of the same hydrogel prior to *in vivo* studies. We also describe here technical methods for *in vivo* delivery to the heart in mice, rats, and pigs. The techniques described in this paper can also be applied to the delivery of injectable hydrogels in other clinical applications, as well as for the evaluation of injectable hydrogels as printing bioinks.

■ ASSOCIATED CONTENT

Supporting Information

The Supporting Information is available free of charge on the ACS Publications website at DOI: [10.1021/acsbiomaterials.7b00734](https://doi.org/10.1021/acsbiomaterials.7b00734).

MATLAB code, schematics of synthesis, rheological data, cell viability measurements, photos of *in vivo* hydrogel injection, and video descriptions (PDF)

Videos S1, demonstration of *in vivo* hydrogel injection in mice (MPG)

Video S2, demonstration of *in vivo* hydrogel injection in rats (MPG)

Video S3, demonstration of *in vivo* hydrogel injection in pigs (MPG)

■ AUTHOR INFORMATION

Corresponding Author

*E-mail: burdick2@seas.upenn.edu. Phone: (215) 898-8537. Fax: (215) 573-2071 (J.A.B.).

ORCID

Jason A. Burdick: [0000-0002-2006-332X](https://orcid.org/0000-0002-2006-332X)

Notes

The authors declare no competing financial interest.

Author Contributions

[†]M.H.C. and L.L.W. contributed equally to this work and are considered cofirst authors. The manuscript was written through contributions of all authors. All authors have given approval to the final version of the manuscript.

■ ACKNOWLEDGMENTS

This work was made possible by financial support from the American Heart Association through an established investigator award (J.A.B.) and predoctoral fellowships (M.H.C., L.L.W.) and the National Institutes of Health (T32 AR007132, F30 HL134255, R01 HL135090).

■ REFERENCES

- (1) Guvendiren, M.; Lu, H. D.; Burdick, J. A. Shear-thinning hydrogels for biomedical applications. *Soft Matter* **2012**, *8* (2), 260–272.
- (2) Burdick, J. A.; Prestwich, G. D. Hyaluronic acid hydrogels for biomedical applications. *Adv. Mater.* **2011**, *23* (12), H41–56.
- (3) Tous, E.; Purcell, B.; Ifkovits, J. L.; Burdick, J. A. Injectable Acellular Hydrogels for Cardiac Repair. *J. Cardiovasc. Transl. Res.* **2011**, *4* (5), S28–S42.
- (4) Rodell, C. B.; MacArthur, J. W.; Dorsey, S. M.; Wade, R. J.; Wang, L. L.; Woo, Y. J.; Burdick, J. A. Shear-Thinning Supramolecular Hydrogels with Secondary Autonomous Covalent Crosslinking to Modulate Viscoelastic Properties *In Vivo*. *Adv. Funct. Mater.* **2015**, *25* (4), 636–644.
- (5) Khetan, S.; Burdick, J. A. Cellular Encapsulation in 3D Hydrogels for Tissue Engineering. *J. Visualized Exp.* **2009**, No. 32, e1590.
- (6) Gaffey, A. C.; Chen, M. H.; Venkataraman, C. M.; Trubelja, A.; Rodell, C. B.; Dinh, P. V.; Hung, G.; MacArthur, J. W.; Soopan, R. V.; Burdick, J. A.; et al. Injectable shear-thinning hydrogels used to deliver endothelial progenitor cells, enhance cell engraftment, and improve ischemic myocardium. *J. Thorac. Cardiovasc. Surg.* **2015**, *150* (5), 1268–1277.
- (7) Purcell, B. P.; Lobb, D.; Charati, M. B.; Dorsey, S. M.; Wade, R. J.; Zellars, K. N.; Doviak, H.; Pettaway, S.; Logdon, C. B.; Shuman, J. A.; et al. Injectable and bioresponsive hydrogels for on-demand matrix metalloproteinase inhibition. *Nat. Mater.* **2014**, *13* (6), 653–661.
- (8) Rodell, C. B.; Wade, R. J.; Purcell, B. P.; Dusaj, N. N.; Burdick, J. A. Selective Proteolytic Degradation of Guest–Host Assembled, Injectable Hyaluronic Acid Hydrogels. *ACS Biomater. Sci. Eng.* **2015**, *1* (4), 277–286.
- (9) Huynh, C. T.; Nguyen, M. K.; Tonga, G. Y.; Longé, L.; Rotello, V. M.; Alsborg, E. Photocleavable Hydrogels for Light-Triggered siRNA Release. *Adv. Healthcare Mater.* **2016**, *5* (3), 305–310.
- (10) Highley, C. B.; Kim, M.; Lee, D.; Burdick, J. A. Near-infrared light triggered release of molecules from supramolecular hydrogel-nanorod composites. *Nanomedicine* **2016**, *11*, 1579.
- (11) Yang, J. A.; Yeom, J.; Hwang, B. W.; Hoffman, A. S.; Hahn, S. K. *In situ*-forming injectable hydrogels for regenerative medicine. *Prog. Polym. Sci.* **2014**, *39* (12), 1973–1986.
- (12) Hillel, A. T.; Unterman, S.; Nahas, Z.; Reid, B.; Coburn, J. M.; Axelman, J.; Chae, J. J.; Guo, Q.; Trow, R.; Thomas, A.; et al. Photoactivated composite biomaterial for soft tissue restoration in rodents and in humans. *Sci. Transl. Med.* **2011**, *3* (93), 93ra67.
- (13) Martens, T. P.; Godier, A. F. G.; Parks, J. J.; Wan, L. Q.; Koeckert, M. S.; Eng, G. M.; Hudson, B. I.; Sherman, W.; Vunjak-Novakovic, G. Percutaneous cell delivery into the heart using hydrogels polymerizing *in situ*. *Cell Transplant.* **2009**, *18* (3), 297–304.
- (14) Lu, H. D.; Soranno, D. E.; Rodell, C. B.; Kim, I. L.; Burdick, J. A. Secondary Photocrosslinking of Injectable Shear-Thinning Dock-and-Lock Hydrogels. *Adv. Healthcare Mater.* **2013**, *2* (7), 1028–1036.

- (15) Wang, L. L.; Sloand, J. N.; Gaffey, A. C.; Venkataraman, C. M.; Wang, Z.; Trubelja, A.; Hammer, D. A.; Atluri, P.; Burdick, J. A. Injectable, Guest–Host Assembled Polyethylenimine Hydrogel for siRNA Delivery. *Biomacromolecules* **2017**, *18* (1), 77–86.
- (16) Li, Y.; Fan, L.; Liu, S.; Liu, W.; Zhang, H.; Zhou, T.; Wu, D.; Yang, P.; Shen, L.; Chen, J.; et al. The promotion of bone regeneration through positive regulation of angiogenic-osteogenic coupling using microRNA-26a. *Biomaterials* **2013**, *34* (21), 5048–5058.
- (17) Ifkovits, J. L.; Tous, E.; Minakawa, M.; Morita, M.; Robb, J. D.; Koomalsingh, K. J.; Gorman, J. H.; Gorman, R. C.; Burdick, J. A. Injectable hydrogel properties influence infarct expansion and extent of postinfarction left ventricular remodeling in an ovine model. *Proc. Natl. Acad. Sci. U. S. A.* **2010**, *107* (25), 11507–11512.
- (18) Ouyang, L.; Highley, C. B.; Rodell, C. B.; Sun, W.; Burdick, J. A. 3D Printing of Shear-Thinning Hyaluronic Acid Hydrogels with Secondary Cross-Linking. *ACS Biomater. Sci. Eng.* **2016**, *2* (10), 1743–1751.
- (19) Highley, C. B.; Rodell, C. B.; Burdick, J. A. Direct 3D Printing of Shear-Thinning Hydrogels into Self-Healing Hydrogels. *Adv. Mater.* **2015**, *27* (34), 5075–5079.
- (20) Haines-Butterick, L.; Rajagopal, K.; Branco, M.; Salick, D.; Rughani, R.; Pilarz, M.; Lamm, M. S.; Pochan, D. J.; Schneider, J. P. Controlling hydrogelation kinetics by peptide design for three-dimensional encapsulation and injectable delivery of cells. *Proc. Natl. Acad. Sci. U. S. A.* **2007**, *104* (19), 7791–7796.
- (21) Bakota, E. L.; Sensoy, O.; Ozgur, B.; Sayar, M.; Hartgerink, J. D. Self-assembling multidomain peptide fibers with aromatic cores. *Biomacromolecules* **2013**, *14* (5), 1370–1378.
- (22) Wong Po Foo, C. T. S.; Lee, J. S.; Mulyasmita, W.; Parisi-Amon, A.; Heilshorn, S. C. Two-component protein-engineered physical hydrogels for cell encapsulation. *Proc. Natl. Acad. Sci. U. S. A.* **2009**, *106* (52), 22067–22072.
- (23) Cai, L.; Dewi, R. E.; Heilshorn, S. C. Injectable Hydrogels with In Situ Double Network Formation Enhance Retention of Transplanted Stem Cells. *Adv. Funct. Mater.* **2015**, *25* (9), 1344–1351.
- (24) Hong, S.; Sycks, D.; Chan, H. F.; Lin, S.; Lopez, G. P.; Guilak, F.; Leong, K. W.; Zhao, X. 3D Printing of Highly Stretchable and Tough Hydrogels into Complex, Cellularized Structures. *Adv. Mater.* **2015**, *27* (27), 4035–4040.
- (25) Gupta, D.; Tator, C. H.; Shoichet, M. S. Fast-gelling injectable blend of hyaluronan and methylcellulose for intrathecal, localized delivery to the injured spinal cord. *Biomaterials* **2006**, *27* (11), 2370–2379.
- (26) Wang, Q.; Wang, J.; Lu, Q.; Detamore, M. S.; Berkland, C. Injectable PLGA based colloidal gels for zero-order dexamethasone release in cranial defects. *Biomaterials* **2010**, *31* (18), 4980–4986.
- (27) Zhao, S.-P.; Xu, W.-L. Thermo-sensitive hydrogels formed from the photocrosslinkable polypseudorotaxanes consisting of β -cyclodextrin and Pluronic F68/PCL macromer. *J. Polym. Res.* **2010**, *17* (4), 503–510.
- (28) Khodaverdi, E.; Mirzazadeh Tekie, F. S.; Hadizadeh, F.; Esmaeel, H.; Mohajeri, S. A.; Sajadi Tabassi, S. A.; Zohuri, G. Hydrogels composed of cyclodextrin inclusion complexes with PLGA-PEG-PLGA triblock copolymers as drug delivery systems. *AAPS PharmSciTech* **2014**, *15* (1), 177–188.
- (29) van de Manacker, F.; van der Pot, M.; Vermonden, T.; van Nostrum, C. F.; Hennink, W. E. Self-Assembling Hydrogels Based on β -Cyclodextrin/Cholesterol Inclusion Complexes. *Macromolecules* **2008**, *41*, 1766–1773.
- (30) Rodell, C. B.; Kaminski, A. L.; Burdick, J. A. Rational Design of Network Properties in Guest–Host Assembled and Shear-Thinning Hyaluronic Acid Hydrogels. *Biomacromolecules* **2013**, *14* (11), 4125–4134.
- (31) Wang, L. L.; Sloand, J. N.; Gaffey, A. C.; Venkataraman, C. M.; Wang, Z.; Trubelja, A.; Hammer, D. A.; Atluri, P.; Burdick, J. A. Injectable, Guest-Host Assembled Polyethylenimine Hydrogel for siRNA Delivery. *Biomacromolecules* **2017**, *18* (1), 77–86.
- (32) Wang, H.; Zhu, D.; Paul, A.; Cai, L.; Enejder, A.; Yang, F.; Heilshorn, S. C. Covalently Adaptable Elastin-Like Protein-Hyaluronic Acid (ELP-HA) Hybrid Hydrogels with Secondary Thermoresponsive Crosslinking for Injectable Stem Cell Delivery. *Adv. Funct. Mater.* **2017**, *27* (28), 1605609.
- (33) Huang, W.; Wang, Y.; Chen, Y.; Zhao, Y.; Zhang, Q.; Zheng, X.; Chen, L.; Zhang, L. Strong and Rapidly Self-Healing Hydrogels: Potential Hemostatic Materials. *Adv. Healthcare Mater.* **2016**, *5* (21), 2813–2822.
- (34) Grover, G. N.; Braden, R. L.; Christman, K. L. Oxime cross-linked injectable hydrogels for catheter delivery. *Adv. Mater.* **2013**, *25* (21), 2937–2942.
- (35) Rodell, C. B.; Lee, M. E.; Wang, H.; Takebayashi, S.; Takayama, T.; Kawamura, T.; Arkles, J. S.; Dusaj, N. N.; Dorsey, S. M.; Witschey, W. R. T.; et al. Injectable Shear-Thinning Hydrogels for Minimally Invasive Delivery to Infarcted Myocardium to Limit Left Ventricular Remodeling. *Circ.: Cardiovasc. Interventions* **2016**, *9* (10), e004058.
- (36) Aguado, B. A.; Mulyasmita, W.; Su, J.; Lampe, K. J.; Heilshorn, S. C. Improving Viability of Stem Cells During Syringe Needle Flow Through the Design of Hydrogel Cell Carriers. *Tissue Eng., Part A* **2012**, *18* (7–8), 806–815.
- (37) Dubbin, K.; Tabet, A.; Heilshorn, S. Quantitative criteria to benchmark new and existing bio-inks for cell compatibility. *Biofabrication* **2017**, *9* (4), 044102.
- (38) Malda, J.; Visser, J.; Melchels, F. P.; Jüngst, T.; Hennink, W. E.; Dhert, W. J. A.; Groll, J.; Hutmacher, D. W. 25th Anniversary Article: Engineering Hydrogels for Biofabrication. *Adv. Mater.* **2013**, *25* (36), 5011–5028.
- (39) Loebel, C.; Rodell, C. B.; Chen, M. H.; Burdick, J. A. Shear-thinning and self-healing hydrogels as injectable therapeutics and for 3D-printing. *Nat. Protoc.* **2017**, *12* (8), 1521–1541.
- (40) Chen, D. T. N.; Wen, Q.; Janmey, P. A.; Crocker, J. C.; Yodh, A. G. Rheology of soft materials. *Annu. Rev. Condens. Matter Phys.* **2010**, *1* (1), 301–322.
- (41) Öhrlund, Å.; Edsman, K.; Stuesson, C.; Nord, L.; Kenne, A. H.; Näsström, J. Extrusion Force and Syringe Dimensions of Two Hyaluronic Acid Dermal Fillers. *8th Anti-aging Medicine World Congress*; Monte-Carlo, Monaco, April 8–10, 2008; EuroMediCom: Paris, 2010.
- (42) Vo, A.; Doumit, M.; Rockwell, G. The Biomechanics and Optimization of the Needle-Syringe System for Injecting Triamcinolone Acetonide into Keloids. *J. Med. Eng.* **2016**, *2016*, 5162394.
- (43) Yushkevich, P. A.; Piven, J.; Hazlett, H. C.; Smith, R. G.; Ho, S.; Gee, J. C.; Gerig, G. User-guided 3D active contour segmentation of anatomical structures: Significantly improved efficiency and reliability. *NeuroImage* **2006**, *31* (3), 1116–1128.
- (44) Seif-Naraghi, S. B.; Singelyn, J. M.; Salvatore, M. A.; Osborn, K. G.; Wang, J. J.; Sampat, U.; Kwan, O. L.; Strachan, G. M.; Wong, J.; Schup-Magoffin, P. J.; et al. Safety and efficacy of an injectable extracellular matrix hydrogel for treating myocardial infarction. *Sci. Transl. Med.* **2013**, *5* (173), 173ra25.
- (45) Macarthur, J. W.; Purcell, B. P.; Shudo, Y.; Cohen, J. E.; Fairman, A.; Trubelja, A.; Patel, J.; Hsiao, P.; Yang, E.; Lloyd, K.; et al. Sustained release of engineered stromal cell-derived factor 1-alpha from injectable hydrogels effectively recruits endothelial progenitor cells and preserves ventricular function after myocardial infarction. *Circulation* **2013**, *128* (Suppl 1), S79–S86.
- (46) Shao, Y.; Redfors, B.; Omerovic, E. Modified Technique for Coronary Artery Ligation in Mice. *J. Visualized Exp.* **2013**, No. 73, e3093.
- (47) Munz, M. R.; Faria, M. A.; Monteiro, J. R.; Aguas, A. P.; Amorim, M. J. Surgical porcine myocardial infarction model through permanent coronary occlusion. *Comp. Med.* **2011**, *61* (5), 445–452.
- (48) Koudstaal, S.; Jansen of Lorkeers, S.; Gho, J. M. I. H.; van Hout, G. P. J.; Jansen, M. S.; Gründeman, P. F.; Pasterkamp, G.; Doevendans, P. A.; Hofer, I. E.; Chamuleau, S. A. J. Myocardial infarction and functional outcome assessment in pigs. *J. Visualized Exp.* **2014**, No. 86, e51269.
- (49) McCall, F. C.; Telukuntla, K. S.; Karantalis, V.; Suncion, V. Y.; Heldman, A. W.; Mushtaq, M.; Williams, A. R.; Hare, J. M. Myocardial

infarction and intramyocardial injection models in swine. *Nat. Protoc.* **2012**, *7* (8), 1479–1496.

(50) Camacho, P.; Fan, H.; Liu, Z.; He, J.-Q. Small mammalian animal models of heart disease. *Am. J. Cardiovasc. Dis.* **2016**, *6* (3), 70–80.

(51) Breckenridge, R. Heart failure and mouse models. *Dis. Models & Mech.* **2010**, *3* (3–4), 138–143.

(52) Gao, E.; Lei, Y. H.; Shang, X.; Huang, Z. M.; Zuo, L.; Boucher, M.; Fan, Q.; Chuprun, J. K.; Ma, X. L.; Koch, W. J. A novel and efficient model of coronary artery ligation and myocardial infarction in the mouse. *Circ. Res.* **2010**, *107* (12), 1445–1453.

(53) Kumar, M.; Kasala, E. R.; Bodduluru, L. N.; Dahiya, V.; Sharma, D.; Kumar, V.; Lahkar, M. Animal models of myocardial infarction: Mainstay in clinical translation. *Regul. Toxicol. Pharmacol.* **2016**, *76*, 221–230.

(54) Wu, Y.; Yin, X.; Wijaya, C.; Huang, M.-H.; McConnell, B. K. Acute Myocardial Infarction in Rats. *J. Visualized Exp.* **2011**, No. 48, e2464.

(55) Dixon, J. A.; Spinale, F. G. Large animal models of heart failure; A critical link in the translation of basic science to clinical practice. *Circ. Heart Fail.* **2009**, *2*, 262–271.

(56) Tsang, H. G.; Rashdan, N. A.; Whitelaw, C. B. A.; Corcoran, B. M.; Summers, K. M.; MacRae, V. E. Large animal models of cardiovascular disease. *Cell Biochem. Funct.* **2016**, *34* (3), 113–132.

(57) Li, J.; Illeperuma, W. R. K.; Suo, Z.; Vlassak, J. J. Hybrid hydrogels with extremely high stiffness and toughness. *ACS Macro Lett.* **2014**, *3* (6), 520–523.

(58) Rodell, C. B.; Dusaj, N. N.; Highley, C. B.; Burdick, J. A. Injectable and Cytocompatible Tough Double-Network Hydrogels through Tandem Supramolecular and Covalent Crosslinking. *Adv. Mater.* **2016**, *28* (38), 8419–8424.

(59) Neuman, B. J.; Radcliff, K.; Rihn, J. Cauda Equina Syndrome After a TLIF Resulting From Postoperative Expansion of a Hydrogel Dural Sealant. *Clin. Orthop. Relat. Res.* **2012**, *470* (6), 1640–1645.

(60) Hayashi, K.; Okamoto, F.; Hoshi, S.; Katashima, T.; Zujur, D. C.; Li, X.; Shibayama, M.; Gilbert, E. P.; Chung, U.; Ohba, S.; et al. Fast-forming hydrogel with ultralow polymeric content as an artificial vitreous body **2017**, *1*, 0044.

(61) Kamata, H.; Kushiro, K.; Takai, M.; Chung, U.; Sakai, T. Non-Osmotic Hydrogels: A Rational Strategy for Safely Degradable Hydrogels. *Angew. Chem., Int. Ed.* **2016**, *55* (32), 9282–9286.

(62) Abduljabbar, M. H.; Basendwh, M. A. Complications of hyaluronic acid fillers and their managements. *J. Dermatologic Surg.* **2016**, *20* (2), 100–106.